DENTAL MATERIALS 31 (2015) 1279–1289

ScienceDirect

journal homepage: www.intl.elsevierhealth.com/journals/dema

Conversion, shrinkage, water sorption, flexural strength and modulus of re-mineralizing dental composites

A. Aljabo[a], W. Xia[a], S. Liaqat[a], M.A. Khan[a], J.C. Knowles[a], P. Ashley[b], A.M. Young[a,*]

[a] Division of Biomaterials and Tissue Engineering, UCL Eastman Dental Institute, 256 Gray's Inn Road, London WC1X 8LD, UK

[b] Department of Paediatric Dentistry, UCL Eastman Dental Institute, 256 Gray's Inn Road, London WC1X 8LD, UK

ARTICLE INFO

Article history:
Received 3 November 2014
Received in revised form
15 June 2015
Accepted 14 August 2015

Keywords:
Dental composite
Mono and tri calcium phosphate
Antibacterial
Hydroxyapatite
Tooth remineralization
FTIR
Conversion depth
Shrinkage and expansion
Strength
Modulus

ABSTRACT

Objectives. Cure, volumetric changes and mechanical properties were assessed for new dental composites containing chlorhexidine (CHX) and reactive calcium phosphate-containing (CaP) to reduce recurrent caries.

Methods. 20 wt.% of light curable urethane dimethacrylate based liquid was mixed with 80 wt.% glass filler containing 10 wt.% CHX and 0–40 wt.% CaP. Conversion versus depth with 20 or 40 s light exposure was assessed by FTIR. Solidification depth and polymerization shrinkage were determined using ISO 4049 and 17304, respectively. Subsequent volume expansion and biaxial flexural strength and modulus change upon water immersion were determined over 4 weeks. Hydroxyapatite precipitation in simulated body fluid was assessed at 1 week.

Results. Conversion decreased linearly with both depth and CaP content. Average solidification depths were 4.5, 3.9, 3.3, 2.9 and 5.0 with 0, 10, 20, and 40% CaP and a commercial composite, Z250, respectively. Conversions at these depths were 53 ± 2% for experimental materials but with Z250 only 32%. With Z250 more than 50% conversion was achieved only below 1.1 mm. Shrinkage was 3% and 2.5% for experimental materials and Z250, respectively. Early water sorption increased linearly, whilst strength and modulus decreased exponentially to final values when plotted versus square root of time. Maximum volumetric expansion increased linearly with CaP rise and balanced shrinkage at 10–20 wt.% CaP. Strength and modulus for Z250 decreased from 191 to 158 MPa and 3.2 to 2.5 GPa. Experimental composites initial strength and modulus decreased linearly from 169 to 139 MPa and 5.8 to 3.8 GPa with increasing CaP. Extrapolated final values decreased from 156 to 84 MPa and 4.1 to 1.7 GPa. All materials containing CaP promoted hydroxyapatite precipitation.

Significance. The lower surface of composite restorations should both be solid and have greater than 50% conversion. The results, therefore, suggest the experimental composite

Abbreviations: CHX, chlorhexidine; CaP, calcium phosphate; UDMA, urethane dimethacrylate; TEGDMA, triethylene glycol dimethacrylate; HEMA, hydroxyethyl methacrylate; CQ, camphorquinone; DMPT, dimethylparatoluidine; β-TCP, β-tricalcium phosphate; MCPM, monocalcium phosphate monohydrate; FTIR, Fourier transform infrared spectrometer; SEM, scanning electron microscopy.

* *Corresponding author.* Tel.: +44 20 3456 2353.
E-mail address: anne.young@ucl.ac.uk (A.M. Young).

http://dx.doi.org/10.1016/j.dental.2015.08.149

may be placed in much thicker layers than Z250 and have reduced unbounded cytotoxic monomer. Experimental materials with 10–20 wt.% additionally have volumetric expansion to compensate shrinkage, antibacterial and re-mineralizing components and competitive mechanical properties.

1. Introduction

Dental caries is caused by bacteria producing acid that then dissolves the hydroxyapatite mineral in the tooth. In order to minimize disease progression, restore function and allow effective biofilm removal, infected tissue is excavated and replaced with a filling material. Following the recent signing and future multinational ratification of the Minamata agreement on mercury, phasing out of amalgam fillings will become likely. Dental composites will then be the main direct tooth restorative material. Unfortunately composites generally require replacing more often and are technically more difficult to place [1–3].

Dental composites consist of filled light curable dimethacrylate monomers. Their failure can be via fracture due to low strength but is more commonly nowadays caused by recurrent caries following composite debonding from the tooth structures. This can result from lack of composite antibacterial action and shrinkage during setting. Resultant micro-gap formation allows bacterial penetration, secondary caries and continuing hydroxyapatite dissolution beneath the composite restoration [1,4].

Many studies have included amorphous calcium phosphate or brushite (dicalcium phosphate dihydrate) particles in dental composite formulations. The aim was to promote surrounding dentin remineralization [5–8]. The low solubility of these calcium phosphates however, could potentially limit this benefit. More recently, mixtures of reactive hydrophilic and hydrophobic calcium phosphates were included in antibacterial chlorhexidine-releasing composites [2,9]. Hydrophilic, water soluble MCPM enhanced rapid water sorption induced swelling which promotes expansion to compensate polymerization shrinkage and effective antibacterial chlorhexidine release. Additionally, surface MCPM readily dissolved. This could potentially supersaturate dentinal fluid and force hydroxyapatite precipitation. In the composite bulk, however, MCPM reacted with βTCP to form less soluble brushite crystals. This reaction can help bind absorbed water. Unbound water would otherwise reduce long-term strength through hydrolysing glass silane surfaces or plasticizing the polymer phase [2].

Previous studies using reactive calcium phosphates and chlorhexidine in composites as the only fillers resulted in excessive expansion and decline in strength [2,9]. Combining more conventional fillers with reactive calcium phosphates partially overcame these issues. Lack of refractive index matching, however, meant formulations had to be cured through mixing of alternative chemical cure initiators with an activator instead of by light exposure [10]. Furthermore, neither of these studies considered cure variation with depth, long term strength reduction or modulus.

High degree of monomer conversion is essential for optimal physical properties and to reduce cytotoxic risks but it does increase polymerization shrinkage [3,11]. High light penetration depth is also required for placement in deeper fillings. The following new study aim was therefore to compare conversion versus depth, volumetric changes and mechanical properties of new light curable composites with reactive calcium phosphates and chlorhexidine. Volumetric studies included both polymerization shrinkage and subsequent expansion that occurs due to water sorption. Re-mineralizing properties have been assessed using a method more commonly employed to investigate bone cement.

2. Materials and methods

In the following, urethane dimethacrylate (UDMA) was used as the base monomer with triethylene glycol dimethacrylate (TEGDMA) and hydroxyethyl methacrylate (HEMA) as diluents. Relative levels were pre-optimized to allow high powder content and low shrinkage whilst ensuring rheological characteristics comparable with commercial composites. Camphorquinone (CQ) and dimethylparatoluidine (DMPT) were employed as initiator and activator, respectively. The base glass was chosen due to its close refractive index (0.52) match with the monomer (0.48) to enable good depth of cure. It additionally had high radiopacity due to barium (ratio of Al:Si:Ba oxides of 1:9.5:3 by XRF) to enable detection in dental X-rays. Furthermore, the particle size range (1 to 20 micron diameter by SEM) enabled high filler content. Chlorhexidine and glass fibers levels were fixed but reactive calcium phosphate levels were varied.

2.1. *Composite paste preparation*

Dental pastes were prepared by combining liquid and powder phases at a powder: liquid ratio of 4:1. The light curable liquid phase consisted of UDMA, TEGDMA and HEMA (all from Esstech) with CQ and DMPT (both from Sigma–Aldrich) in the weight ratio of 68:25:5:1:1. The base powder phase was a silane treated barium boro alumino silicate glass (IF 2019 from Sci-pharm). This component contributed 30, 50, 60 or 70 wt.% of the filler. Additional components were borosilicate glass fibers (MO-SCI) and Chlorhexidine diacetate salt hydrate (CHX) (Sigma–Aldrich) fixed at 20 and 10 wt.% of the total filler, respectively. Furthermore, equal masses of β-tricalcium phosphate (Plasma Biotal) and monocalcium phosphate monohydrate (Himed) were included. The combined reactive

calcium phosphate (CaP) content was 0, 10, 20 or 40 wt.% of the total filler. All components of the powder phase were weighed and mixed on a mixing pad before adding the required amount of monomer to form a paste.

2.2. Monomer conversion

To quantify monomer conversion, composite pastes were placed in metal rings (10 mm internal diameter and 1 mm thick) on the centre diamond of a golden gate ATR top-plate (Specac Ltd., UK) in a Fourier transform infrared spectrometer (FTIR) (Perkin Elmer Series 2000, UK). Up to 4 rings were stacked on top of each other to gain samples of 1, 2, 3 and 4 mm depth. The temperature was kept at 37 °C using a 3000 Series RS232 high stability temperature controller (Specac Ltd., UK). The top surface of the sample was covered with acetate sheet to prevent oxygen inhibition of the polymerization process [12]. FTIR spectra of the lower surface of the specimen in contact with the diamond were recorded with a resolution of 4 cm^{-1} for 20 min from 700 to 2000 cm^{-1}. After 1 min, the top surface was exposed to blue light (Demi Plus, Kerr) for 20 or 40 s. Fractional monomer conversion at 1 to 4 mm depth was calculated from the initial and final peak height at 1320 cm^{-1} above background at 1347 cm^{-1} [2].

2.3. Depth of cure (ISO 4049:2009)

To assess depth of cure using the ISO 4049 method, pastes were condensed into metal moulds (4 mm diameter and 6 mm deep) ($n = 3$). After exposure of the top surface to blue light for 20 s or 40 s, the specimen was removed from the mould and any soft material scraped away using a plastic spatula. The depth of the remaining solid specimen, h, was measured. The depth of cure is presented as half of h according to the ISO standard.

2.4. Polymerization shrinkage

2.4.1. Calculated shrinkage

One mole of polymerizing C=C bonds typically gives volumetric shrinkage of 23 cm^3/mol [5]. Total fractional shrinkage, φ, due to the composite polymerization can therefore be estimated from FTIR monomer conversions, using

$$\varphi = 23C\rho\sum_i \frac{n_i x_i}{W_i} \quad (1)$$

where C, monomer conversion (%); ρ, composite density (g/cm^3); n_i, the number of C=C bonds per molecule; w_i, molecular weight (g/mol) of each monomer; x_i, mass fraction of each monomer.

2.4.2. Experimental shrinkage

Polymerization shrinkage was also determined using Archimedes' principle and ISO 17304:2013. This method determines the densities of unpolymerized paste and polymerized discs by measuring their mass in air and water. An analytic balance (AG 204 Mettler Toledo) equipped with a density kit was used.

2.5. Mass and volume change

For composite density, mass change and volume change determination, pastes were placed in metal rings (1 mm deep and 10 mm internal diameter), covered top and bottom with acetate sheet and light cured for 40 s top and bottom to ensure maximum polymerization of the whole disc. Before testing, the resultant composite discs were removed from the moulds and their edges polished to remove any loose chips. Discs were stored in separate sterilin tubes each containing 10 mL of distilled water at 37 °C. After 0,1, 2, 4, 6 h and 1, 2, 4 days and 1, 2, 4 and 6 weeks, specimens mass, volume and density were determined using a density kit and four-figure digital balance as above.

2.6. Biaxial flexural strength and modulus

To assess strength and modulus variation with time, 1 mm thick and 10 mm diameter specimens were prepared as above and stored either dry or for 1 day, 1 week or 1 month in distilled water. Biaxial flexural strength, S, and modulus, E, were determined using a "ball on ring" jig and a universal testing machine (Instron 4502, U.K.) with the following equations:

$$S = \frac{P}{h^2}\left[(1+\mu)\left(0.485\ln\left(\frac{a}{h}\right)+0.52\right)+0.48\right] \quad (2)$$

$$E = 0.502\frac{dP}{dw}\left(\frac{a^2}{h^3}\right) \quad (3)$$

where P, load; h, sample thickness; μ, Poisons ratio taken as 0.3; dP/dw, the gradient of load versus central deflection; a, the support radius.

2.7. Chlorhexidine release

Discs of each composition ($n = 3$) were weighed and immersed in 10 ml of distilled water within sterilin tubes. At different time points up to 6 weeks (2, 4, 6, 24, 168, 336 and 720 h), the specimens were removed and replaced in fresh distilled water. To quantify CHX release, UV spectra of storage solutions were obtained between 190 and 300 nm using a UV 500 spectrometer (Thermo Spectronic, UK). The resulting spectra were compared with calibration graphs created in the same range for solutions of known concentration of CHX to ensure that the CHX was the only component causing absorbance. The amount of CHX release was calculated using peak absorbance at 255 nm between different time periods from each specimen using the following equation:

$$R_t = \frac{A}{g}V \quad (4)$$

where R_t is the amount of CHX in gram, A is the absorbance at 255 nm, g is the gradient of a calibration curve of absorbance versus CHX concentration and V is the storage solution

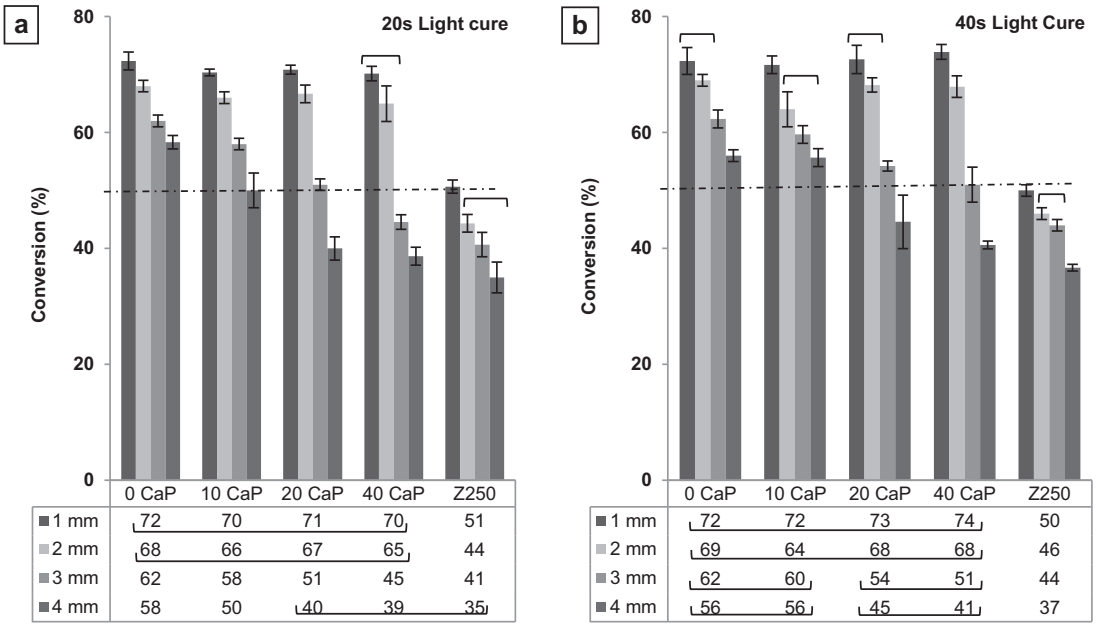

Fig. 1 – Lower surface monomer conversion for composites of 1, 2, 3 or 4 mm depth and containing 0, 10, 20 or 40 wt.% reactive calcium phosphate: (a) 20 s of curing, (b) 40 s of curing. Dotted line indicates a critical conversion of 50% below which samples must contain some monomers with two unreacted methacrylate double bonds. Continuous lines indicate the only data that is not significantly different. (Error bars are 95% confidence interval, $n = 3$).

volume. The percentage cumulative amount of drug release R_c at time t is given by

$$R_c = \frac{100\sum_0^t R_t}{W_c} \quad (5)$$

W_c is the weight of CHX incorporated in a given specimen in gram.

2.8. Hydroxyapatite precipitation in simulated body fluid

To confirm the ability of the materials to promote hydroxyapatite formation, one sample of each material was placed in SBF (as in ISO 23317:2007) for 1 week. After sputter coating with gold–palladium, samples were analyzed using SEM with EDAX (JEOL 5410 LV).

2.9. Data analysis

One-way ANOVA was performed to detect the significant effects of the variables. Tukey's multiple comparison test was used to determine significant differences between specific groups. Sample repetition number was 6 for mechanical tests, polymerization shrinkage and density studies but 3 for all other measurements. Linest (Microsoft excel) was used to fit linear equations, obtain gradients, intercepts, R squared values and 95% confidence intervals. The latter are provided as error bars on graphs and in parentheses with equations. Linest was first applied assuming a non-zero intercept. If the intercept was smaller than its estimated 95% confidence interval, the analysis was repeated assuming a zero intercept.

3. Results

3.1. Monomer conversion

Monomer conversions at the bottom of specimens after curing from the top surface for 20 s or 40 s are illustrated versus sample depth in Fig. 1. Monomer conversion at 1 mm and 2 mm depth was ~70% irrespective of the CaP content. At larger depth, 3 mm and 4 mm, however, there was a significant decrease in the monomer conversion due to increasing CaP content ($P < 0.001$).

Multiple linear regressions gave the intercepts and gradients of conversion, C, versus calcium phosphate concentration, C_p, and depth, h, with 20 s curing time as:

$$C(\%)_{C_{p\to 0}} = 78\,(\pm 1)\left[1 - 0.071\,(\pm 0.005)\left(\frac{h}{\text{mm}}\right)\right] \quad R^2 = 0.99 \quad (6)$$

and

$$\frac{dC\,(\%)}{dC_p\,(\text{wt.\%})} = -0.10\,(\pm 0.04)\left(\frac{h}{\text{mm}}\right) \quad R^2 = 0.85 \quad (7)$$

The small 95% confidence intervals provided in brackets confirm conversion decreased significantly with increasing both C_p and h. Doubling light exposure time, however, had no experimentally significant effect. Combining Eqs. (6) and (7), gave the following equation:

$$C\,(\%) = C(\%)_{C_{p\to 0}} + \frac{dC\,(\%)}{dc_p}(c_p) \quad (8)$$

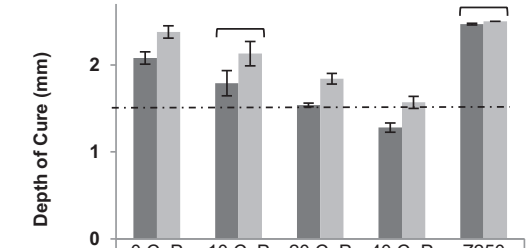

	0 CaP	10 CaP	20 CaP	40 CaP	Z250
20s curing	2.08	1.79	1.54	1.28	2.47
40s curing	2.38	2.13	1.84	1.57	2.5

Fig. 2 – Depth of cure of experimental and commercial composites with 20 and 40 s light exposure. The dotted line indicates the minimum requirement according to the ISO standard. Continuous lines indicate the only data that is not significantly different. (Error bars are 95% confidence interval with $n = 3$).

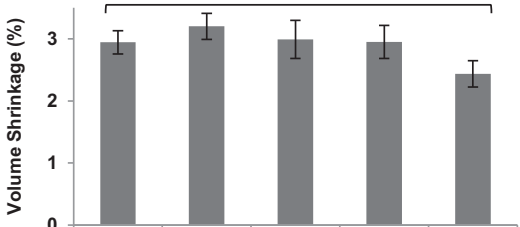

0% CaP	10% CaP	20% CaP	40% CaP	Z250
2.94	3.20	2.99	2.95	2.44

Fig. 3 – Measured polymerization shrinkage of experimental composites with 0 to 40% CaP compared with that of the commercial material Z250. Continuous lines indicate the only data that is not significantly different. (Error bars are 95% confidence interval with $n = 6$).

Using Eqs. (6)–(8) then enables estimation of experimental composite conversions for any depth or composition with more than 20 s light exposure. Linear regression of conversion versus depth for Z250 gave the following equation:

$$C(\%) = 55\,(\pm 1.3)\,[1 - 0.085\,(\pm 0.009)\left(\frac{h}{\text{mm}}\right)] \quad R^2 = 0.98 \qquad (9)$$

The top surface conversion calculated by setting $h = 0$ in Eqs. (6) and (9) indicates that all experimental materials had much higher monomer conversion (78% irrespective of C_p) than Z250 (55%). Gradients of conversion versus depth were not significantly different for the experimental and commercial composites without calcium phosphate. Their decrease with raising calcium phosphate level, however, was significant. From Eqs. (8) and (9), 50% conversion would be achieved at depths, h_{50}, of 5.0, 4.3, 3.7, 2.9 and 1.1 mm depth with 0, 10, 20 and 40 wt.% CaP and Z250, respectively.

3.2. *Depth of cure*

Sample cure depth after 20 s or 40 s light exposure is provided in Fig. 2. With Z250, specimens were solid after cure up to 5 mm depth with either 20 s or 40 s light exposure time. ISO depth of cure was therefore 2.5 mm.

Only the experimental composite containing 40 wt.% CaP cured for 20 s failed to meet the minimum ISO requirement. As with conversion, depth of cure decreased linearly with CaP level ($P < 0.001$). Linear regression gave the experimental ISO depth of cure (1/2 the maximum depth, h_s, at which solidification was observed) as

$$\frac{h_s}{2} = 2.0\,(\pm 0.1)\left[1 - 0.005\,(\pm 0.001)\,\frac{C_p}{\text{wt.\%}}\right] \qquad (10)$$
$$R^2 = 0.96 \quad \text{with} \quad 20 \quad \text{s} \quad \text{cure}$$

$$\frac{h_s}{2} = 2.3\,(\pm 0.1)\left[1 - 0.005\,(\pm 0.001)\,\frac{C_p}{\text{wt.\%}}\right] \qquad (11)$$
$$R^2 = 0.97 \quad \text{with} \quad 40 \quad \text{s} \quad \text{cure}$$

Eqs. (10) and (11) indicated a 15% ((2.3–2)/2) increase in depth of cure with increasing time of exposure from 20 s to 40 s that was independent of calcium phosphate level. Average solidification depths were 4.5, 3.9, 3.3, 2.0 and 5.0 with 0, 10, 20, and 40% CaP and Z250, respectively.

3.3. *Polymerization shrinkage*

Measured polymerization shrinkage results are illustrated in Fig. 3. For 1 mm thick samples the average experimental material shrinkage was 3% and slightly higher than that of Z250 (2.4%). No significant effect of CaP on polymerization shrinkage for experimental formulations ($P > 0.1$).

Experimental material shrinkage was calculated to be 2.5, 3 and 3.5% with average conversions of 55, 65 and 75%, respectively. Shrinkage for Z250 could not be calculated because its exact composition was unknown.

3.4. *Mass and volume change*

Mass and volume change over 6 weeks are shown versus the square root (Sqrt.) of time (hr) in Fig. 4. These plots were linear up to 48 h (Sqrt (time/hr) = 7) with Z250, 0 and 10% CaP, but up to 1 week (Sqrt (time/hr) = 13) with 20 and 40% CaP ($R^2 > 0.98$). This dependence upon time was expected for diffusion controlled water sorption. CaP content has a significant effect on both mass and volume change for experimental formulations ($P < 0.001$).

For Z250 maximum mass and volume change were 1.1 wt.% and 1.5 vol.%, respectively. Z250 density was 2.09 g/cm^3 irrespective of time of immersion. For the experimental materials, linear regression gave the early percentage change in mass, ΔM, and volume, ΔV, as

$$\Delta M\,(\text{wt.\%}) = 0.011\,(\pm 0.002)\left[\frac{C_p}{\text{wt.\%}}\right]\left[\frac{t^{0.5}}{\text{hr}^{0.5}}\right] \quad R^2 = 0.98 \qquad (12)$$

and

$$\Delta V\,(\text{vol.\%}) = 0.020\,(\pm 0.002)\left[\frac{C_p}{\text{wt.\%}}\right]\left[\frac{t^{0.5}}{\text{hr}^{0.5}}\right] \quad R^2 = 0.99 \qquad (13)$$

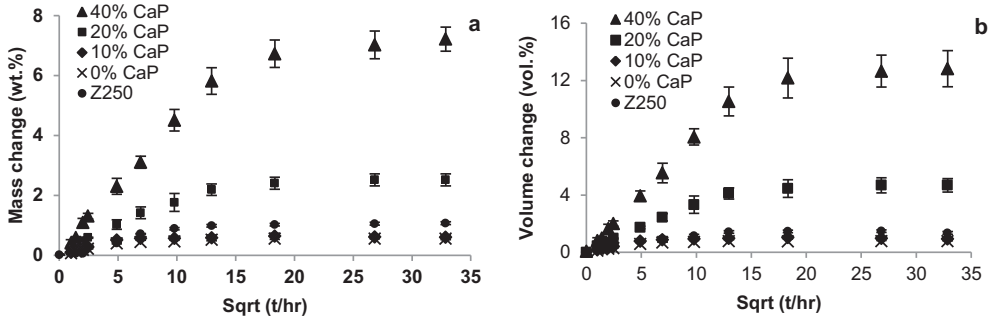

Fig. 4 – (a) Mass change and (b) volume change versus square root (Sqrt) of time for experimental and commercial materials (error bars are estimated 95% CI with $n = 3$).

Early volume change was therefore 1.8 times (0.02/0.011) higher than mass change regardless of CaP content. This was comparable with initial dry composite densities. Between 10 and 40 wt.% CaP, maximum mass and volume changes increased linearly from 0.6 to 7 wt.% and 1 to 13 vol.%, respectively. Linear regression gave

$$\Delta M_{t\to\infty}\,(\text{wt.\%}) = 0.17\,(\pm 0.04)\,\frac{C_p}{\text{wt.\%}} \quad R^2 = 0.96 \tag{14}$$

and

$$\Delta V_{t\to\infty}\,(\text{vol.\%}) = 0.29\,(\pm 0.07)\,\frac{C_p}{\text{wt.\%}} \quad R^2 = 0.96 \tag{15}$$

Eqs. (14) with (15) shows maximum volume change (as $t\to\infty$) was 1.7 (0.29/0.17) times higher than maximum mass change. Integrating Eqs. (12) and (13) and their combination with Eqs. (14) and (15) gives

$$\frac{\Delta M_t}{\Delta M_{t\to\infty}} = 0.065\left(\frac{t}{h}\right)^{0.5} \tag{16}$$

$$\frac{\Delta V_t}{\Delta V_{t\to\infty}} = 0.069\left(\frac{t}{h}\right)^{0.5} \tag{17}$$

When these ratios equal 0.5, t is the time for half maximum change. These "half times" were calculated from Eqs. (16) and (17) to be 59 and 52 h for mass and volume, respectively.

3.5. *Mechanical properties*

Biaxial flexural strength and modulus both decreased with raising CaP level and time in water ($P < 0.001$) (see Fig. 5). Whilst a decrease in strength is a disadvantage, decrease in modulus will increase resilience and energy absorption. It was found that all changes in strength and modulus with time (commercial and experimental) could fit well to the following equations:

$$\ln\frac{(S_t - S_f)}{(S_0 - S_f)} = -0.10\left(\frac{t}{hr}\right)^{0.5} \quad (R^2 = 0.99) \tag{18}$$

$$\ln\frac{(E_t - E_f)}{(E_0 - E_f)} = -0.10\left(\frac{t}{hr}\right)^{0.5} \quad (R^2 = 0.98) \tag{19}$$

Subscripts t, 0 and f indicate strength or modulus at time t, initially ($t\to 0$ and sample is dry) and finally ($t\to\infty$) when the composite has reached equilibrium water sorption. Eqs. (18) and (19) indicate that when $(S_t - S_f)/(S_0 - S_f)$ equals 0.5, t is

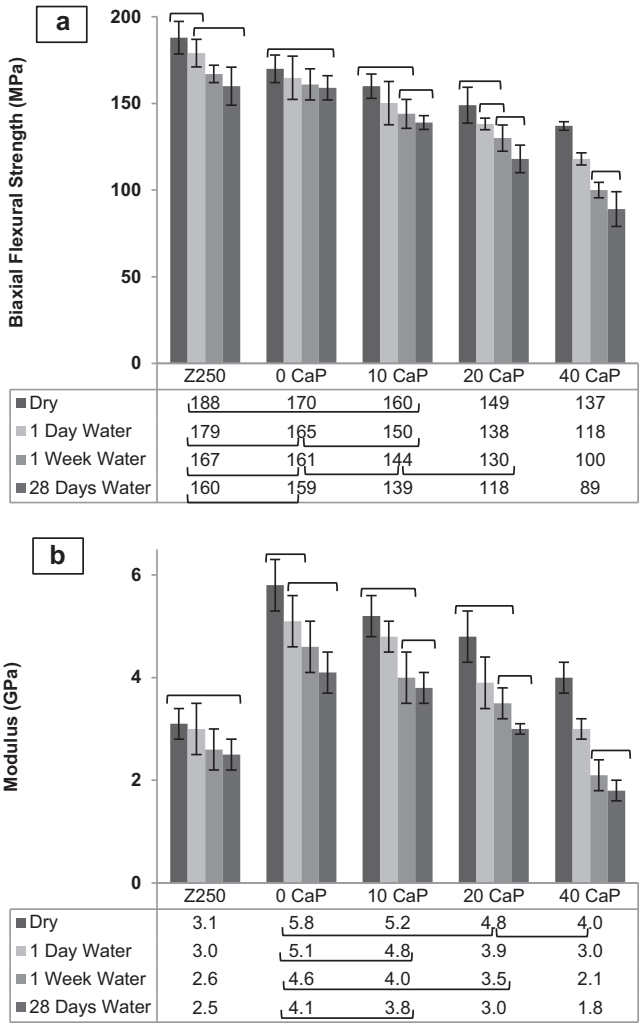

Fig. 5 – (a) Biaxial flexural strength and (b) biaxial flexural modulus of commercial and experimental composites with 0 to 40 wt.% CaP. Continuous lines indicate the only data that is not significantly different. (Error bars are 95% CI with $n = 6$).

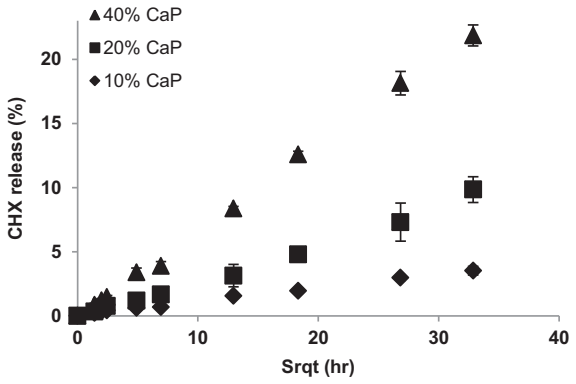

Fig. 6 – CHX release in water from 10, 20 and 40 wt.% CaP formulations up to 6 weeks. (Error bars are 95% CI, $n = 3$).

the time of half maximum reduction in strength or modulus. From Eqs. (16) and (17) this is calculated to be 48 hours for both strength and modulus.

Fitting of Eq. (16) gave initial and final strengths for Z250 of 191 and 158 MPa. Its maximum strength reduction was therefore 17% (33/191 MPa). Linear regression gave the initial and final strengths of the experimental composites verses CaP level C_p as

$$S_0\,(\text{MPa}) = 169\,(\pm 1.6)\left[1 - 0.45\,(\pm 0.05) * 10^{-2}\frac{C_p}{\text{wt.\%}}\right] \quad R^2 = 1.00 \tag{20}$$

and

$$S_f\,(\text{MPa}) = 156\,(\pm 5)\left[1 - 1.1\,(\pm 0.1) * 10^{-2}\frac{C_p}{\text{wt.\%}}\right] \quad R^2 = 0.99 \tag{21}$$

Combining Eqs. (20) and (21) gives fraction change in strength

$$\left(S_0 - S_f\right) = 13\left[1 + 0.077\frac{C_p}{\text{wt.\%}}\right] \tag{22}$$

Eq. (22) shows the maximum reduction in dry strength with increasing CaP level from 0 to 40% was 18%. Eqs. (20) and (21) demonstrate that without calcium phosphate the maximum reduction in strength with time in water was only 8% (13/169 MPa). Eq. (20) shows, however, that increasing CaP level to 10, 20 or 40% causes reduction in strength upon maximum water sorption to rise to 14% (23/161), 21% (33/153) and 38% (53/138), respectively.

Initial and calculated final modulus for Z250 was 3.2 and 2.5 GPa, respectively. Its modulus reduction therefore was 22% (0.7/3.2). Initial and final modulus of composites were found to be given by

$$E_0\,(\text{GPa}) = 5.8\,(\pm 0.1)\left[1 - 0.8\,(\pm 0.1) * 10^{-2}\frac{C_p}{\text{wt.\%}}\right] \quad R^2 = 0.99 \tag{23}$$

and

$$E_f\,(\text{GPa}) = 4.1\,(\pm 0.3)\left[1 - 1.5\,(\pm 0.3) * 10^{-2}\frac{C_p}{\text{wt.\%}}\right] \quad R^2 = 0.98 \tag{24}$$

Subtracting Eqs. (24) from (23) gives

$$\left(E_0 - E_f\right)\,(\text{GPa}) = 1.7 + 0.015\frac{C_p}{\text{wt.\%}} \tag{25}$$

Eq. (23) shows that the addition of calcium phosphate caused a greater maximum reduction in dry modulus of 32%. Eqs. (23) and (25) indicate that without calcium phosphate, the maximum reduction in modulus with time was 30% (1.7/5.8). Eq. (25) shows, however, that increasing CaP level to 10, 20 or 40% caused reduction in modulus to rise to 35% (1.9/5.3), 41% (2.0/4.9) and 58% (2.3/3.9), respectively.

3.6. *Chlorhexidine release*

The amount of CHX release in water was proportional to the square root of time see Fig. 6. This was expected for a diffusion-controlled process. CaP content in the formulations has a significant effect on the CHX release ($P < 0.001$). No CHX release was detected for formulation without CaP.

3.7. *Mineralizing properties*

After 1 week in SBF experimental materials with 10 to 40% CaP had areas coated with balls of crystals (see Fig. 7) that

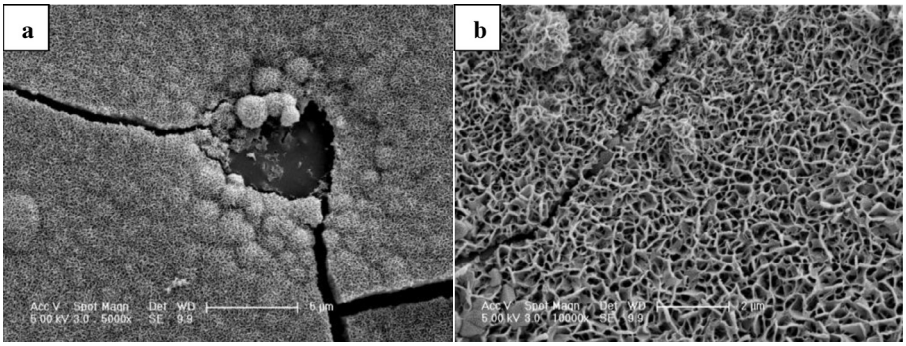

Fig. 7 – SEM images of hydroxyapatite on the surface of composite with 20 wt.% CaP after 1 week in SBF. (a) The composite surface can be seen in centre of the image under the hydroxyapatite crystals. (b) Higher magnification image for the hydroxyapatite crystals.

were shown by EDAX to have a Ca/P ratio of 5/3 as expected for hydroxyapatite. The layer thickness and coverage both increased with raising CaP content. No hydroxyapatite was observed on either Z250 or the composite with no CaP.

4. Discussion

The above results have provided equations that demonstrate how conversion, depth of cure, shrinkage, water sorption, strength and modulus of UDMA based, antibacterial- containing composites vary with reactive calcium phosphate content, sample depth and time.

4.1. Conversion

The above study showed that on the top surface of the experimental composites conversion was much higher (78%) than observed with Z250 (55%) [13]. Higher conversion is generally associated with monomers of lower glass transition temperature, T_g. For BisGMA (the main monomer in Z250), UDMA and TEGDMA these are −8, −35 and −83 °C, respectively [14,15]. With homopolymers without filler BISGMA, UDMA and TEGDMA were found to have maximum conversions of 35, 72 and 83% [16]. The top surface conversions observed in the above new study are therefore as might be expected.

The reduction in conversion versus depth for Z250 observed above is in good agreement with that obtained previously using Raman [17]. In the same study it was shown that high levels of monomer could only be extracted from Z250 below a critical conversion of 50%. This critical concentration is most probably because small monomer molecules can diffuse and polymerize much faster than methacrylates bound into the polymer chains [17]. Therefore, with dimethacrylates there will be few monomers remaining unattached to polymer chains once 50% methacrylate conversion is reached. The above study showed less than 50% conversion was observed for Z250 at all depths below 1 mm. With the experimental composite with no CaP the conversion was well above 50% even at 4 mm depth. Eluted monomers are cytotoxic for pulp and gingival cells. Leaching of uncured monomer has also been implicated in cell alteration and the development of cariogenic bacteria at the interface between the filling and the walls of the cavity [18,19].

The level of conversion decreases with depth due to reduction in activating light intensity. The Beer Lambert law is given by

$$\frac{I}{I_0} = 10^{-\varepsilon[CQ]h} \quad (26)$$

where I_0, intensity of incident light; I, intensity of transmitted light; ε, molar extinction coefficient of CQ (46 cm^{-1}/(mol/L)) [10], [CQ] concentration of CQ in the experimental composites (0.024 mol/L); h, sample depth (mm).

The intensity of transmitted light would therefore be predicted to be 0.36 times the surface incident light at 4 mm depth. Photo bleaching of the CQ may enable slightly greater light transmission than predicted. Reduction in light transmission can also, however, be caused by light scattering [20] due to mismatch in refractive indices of the liquid and any suspended particles. The monomer refractive indices are 1.46, 1.48 and 1.55 for TEGDMA, UDMA, and BISGMA, respectively [21]. Those of the powder components are 1.48, 1.52, 1.63 and 1.66 for glass, MCPM, TCP and CHX. In the experimental composites, the glass and monomers are well matched but addition of increasing levels of TCP is expected to enhance scattering. This explains the reduction in conversion observed with increasing CaP in the above study.

As 50% conversion was observed at much greater depths for the experimental materials (2.9 to 5 mm) than with Z250, the former may be placed in much thicker layers without high risk of monomer leaching. Placement in thicker layers would simplify the restoration process in clinical practise. Typically restorations can be up to 4 mm in depth.

4.2. ISO depth of cure

The ISO depth of cure obtained for Z250 was comparable with that previously observed [17]. From Eq. (9), the calculated monomer conversion for Z250 at the ISO depth of cure (2.5 mm) is only 43%. This suggests that the ISO test may be over estimating the thickness of Z250 layers that can be placed safely from a biocompatibility point of view. Conversely, using Eqs. (6)–(8) with the experimental materials, the conversion at the ISO depth of cure increased linearly from 65 to 69% upon raising the CaP percentage. This suggests that the ISO test may underestimate the thickness of experimental materials that can be placed at one time. This highlights the need for using both conversion and ISO studies to assess depth of cure of dental composites.

The ISO test, unlike the FTIR study showed a significant effect of increasing the time of light exposure from 20 to 40 s. This could be a consequence of extra light exposure only having a significant effect before the materials become hard. From Eqs. (6)–(9) the conversions when the materials become hardened are 55, 52, 52, 51 and 32% with 0, 10, 20 and 40 wt.% CaP and Z250, respectively. In the FTIR studies most conversions were above these values.

4.3. Polymerization shrinkage

Previous studies have shown shrinkage of commercial composites by mercury dilatometry can vary between 2 and 6 vol.% and equal to 2.5% for Z250 [22] in good agreement with the new data above. The measured polymerization shrinkage of the experimental composites (~3%) was well within the range observed for current materials. It was also in good agreement with theory. This gives shrinkage as proportional to conversion, monomer volume fraction, number of methacrylate groups per monomer and inverse average monomer molecular weight.

4.4. Water sorption and mass/volume change

The water sorption of Z250 was recently observed to be between 22 and 28 mg/cm^3 [23,24] The final value of 1.1 wt.% observed in the above new study corresponds with 23 mg/cm^3 which is in good agreement. If water expands the composite then assuming the material behaves ideally it can be shown

by simple rules of mixtures that the fractional volume change will be

$$V = \frac{1}{((1/M) - 1)(\rho_2/\rho_1) + 1} \quad (27)$$

This for small fractional changes in mass simplifies to

$$V = \frac{\rho_2}{\rho_1} M \quad (28)$$

where V is volume change, M is mass change, ρ_1 and ρ_2 are the density of sample and water, respectively.

As the density of water is one the volume change of the composite is approximately equal to the mass change times its density. Alternatively, if the water occupies pores, then mass will increase but volume remain unchanged. The ratio of maximum volume divided by mass change observed above was less than Z250 density suggesting a combination of these 2 effects. With the new composites the ratio of volume divided by mass was equal to density. This suggests most of the change is a result of expansion and there may be fewer pores to fill. From Fig. 4b, a formulation with between 10% and 20% CaP can be expected to have volume expansion of ~3% upon water sorption, to balance the 3% polymerization shrinkage shown in Fig. 3.

The above studies showed the maximum water sorption was proportional to the CaP percentage. The presence of hydrophilic mono-calcium phosphate attracts water into the composite. Previous work has shown this water enables MCPM reaction with TCP to form brushite [9].

The chemical reaction for brushite formation is:(29) $Ca(H_2PO_4)_2 \times H_2O + \beta\text{-}Ca_3(PO_4)_2 + 7H_2O$ ® $4CaHPO_4 \times 2H_2O$

This demonstrates that 1 g of MCPM requires 0.5 g of H_2O to fully react. For the experimental composites this would correspond with 1 wt.% CaP requiring 0.20 wt.% increase in mass due to water sorption. Eq. (14) shows that 85% (0.17/0.2) of the water required for full MCPM conversion to brushite is absorbed irrespective of CaP level. The unreacted MCPM may be released to enhance remineralization.

According to Fick's law of diffusion [25]

$$\frac{\Delta M_t}{\Delta M_{t\to\infty}} = 2\sqrt{\frac{Dt}{\pi h^2}} \quad (30)$$

where D, diffusion coefficient of water into the composite (cm^2/s); t, time (s); h, sample thickness (cm).

Combining this with Eq. (16) gives

$$2\sqrt{\frac{D}{\pi h^2}} = 0.065/h \quad (28)$$

Since the sample thickness h was 0.1 cm this gives $D = 9.2 \times 10^{-14}\ m^2/s$ which is in the range expected from previous values for composite water sorption [26]. From Eq. (14) this diffusion coefficient is independent of CaP content. This suggests the composition of the matrix polymer phase is key in determining the water sorption rate.

Water sorption is also influenced by the affinity of polymer matrix for water. This depends on the quantity of hydrophilic groups (e.g. hydroxyl groups) [27]. Hydrophilic monomer HEMA was shown to induce water sorption leading to expansion of polymer matrix [28]. HEMA makes up 5 wt% of the monomer in the experimental formulation and it is expected to contribute to mass and volume increase. In addition, CHX release may lead to formation of pores in the composite structure. This could further contribute to the mass increase.

4.5. *Mechanical properties*

Commercial composites have been shown to have flexural strength between 100 to 180 MPa with Z250 being the highest [24]. A recent study showed that unfilled UDMA/TEGDMA polymers have higher strength than BISGMA/TEGDMA polymers [29]. The filled experimental composite without CaP in the above study, however, had slightly lower initial strength than Z250. This could be partially attributed to differing inorganic fillers and quality of interface bonding between the fillers and resin [30]. Fillers in Z250 are a mixture of finer zirconium and silicon oxide instead of barium aluminosilicate in the new composites [24]. Upon varying UDMA/TEGDMA ratio maximum unfilled polymer strength has been observed at a 50/50 ratio. Too much TEGDMA, however, would give very high shrinkage [29]. In the above study, therefore, it was fixed at 75/25 UDMA/TEGDMA.

The similarity of times of half maximum change in volume, strength and modulus suggest all are caused by increasing water sorption. Exponential decline in the strength and modulus versus square root of time may be a consequence of increasing micro porosity upon water sorption [31]. The decline in biaxial flexural strength of Z250 observed in the above study was comparable with previous studies [32]. The lower percentage reduction of the experimental composite without CaP could be a consequence of the greater conversion and crosslinking.

The linear decline in dry strength upon increasing CaP (up to maximum of 18% reduction) is possibly due to a lack of coupling agent between the CaP fillers and polymer matrix phase. With increasing CaP from 0 to 40 wt.% CaP, the percentage reduction in strength upon immersion increased linearly from 8 to 38%. This may be in part due to increased water sorption. Furthermore, there may be increasing porosity due to the required release of some unreacted MCPM to promote mineralization.

The modulus of Z250 was initially 45% of the new composite with no CaP. This may be a consequence of the much higher crosslinking in the experimental material. In Z250, lack of crosslinking will allow entangled polymer chains to be pulled apart. In the experimental materials the high level of crosslinking will prevent this. The high reduction in modulus of the experimental composite with no CaP (30%) compared with Z250 (22%) upon placement in water may be a consequence of the polymer chains being more plasticized. The further reduction in modulus upon adding CaP and subsequent water immersion could be due to lack of reactive filler matrix bonding and increasing porosity, respectively.

4.6. *Chlorhexidine release*

Previous studies have incorporated CHX into dental restoratives [33,34] to provide antibacterial activity. CHX was shown

to significantly decrease bacterial count, biofilm formation and lactic acid production [35,36].

CHX release from experimental formulations into water was proportional to Sqrt. of time as expected for a diffusion-controlled process. Upon raising the CaP levels in the formulations, CHX release was substantially increased, which is in good agreement with a previous study [9]. This could be due to increased water sorption induced with CaP in the samples. This absorbed water dissolves CHX enabling its release to the surroundings. It is, therefore, expected that no CHX release to be detected for formulation with 0% CaP.

4.7. *Mineralizing properties*

Studies have shown that dentinal fluid under a restoration is similar in composition to SBF [37]. The ability of the CaP containing materials to promote hydroxyapatite precipitation would enable them to help seal dentin tubules and re-mineralize collagen.

5. Conclusion

This study has produced dental composites containing antibacterial chlorhexidine and re-mineralizing calcium phosphates with superior cure, expansion to compensate shrinkage and with < than 20% CaP comparable mechanical properties to commercial materials. These features would enable easier placement of deeper tooth restorations and reduction in recurrent caries without enhancement of failure due to fracture.

Acknowledgements

EPSRC (EP/I022341/1), Davis Schottlander & Davis Ltd, the Libyan Government provided financial support of W. Xia and A. Aljabo. ESSCHEM, Himed and Ozics have supplied monomers, CaP and silica fillers, respectively.

REFERENCES

[1] Bernardo M. Survival and reasons for failure of amalgam versus composite posterior restorations placed in a randomized clinical trial. J Am Dent Assoc 2007;138:775.
[2] Mehdawi I, Pratten J, Spratt DA, Knowles JC, Young AM. High strength re-mineralizing, antibacterial dental composites with reactive calcium phosphates. Dent Mater 2013;29:473–84.
[3] Krifka S, Hiller K-A, Bolay C, Petzel C, Spagnuolo G, Reichl F-X, et al. Function of MAPK and downstream transcription factors in monomer-induced apoptosis. Biomaterials 2012;33:740–50.
[4] Gama-Teixeira A, Simionato MRL, Elian SN, Sobral MAP, Luz MAAdC. *Streptococcus mutans*-induced secondary caries adjacent to glass ionomer cement, composite resin and amalgam restorations in vitro. Braz Oral Res 2007;21:368–74.
[5] Regnault WF, Icenogle TB, Antonucci JM, Skrtic D. Amorphous calcium phosphate/urethane methacrylate resin composites. I. Physicochemical characterization. J Mater Sci: Mater Med 2008;19:507–15.
[6] Xu H, Weir M, Sun L, Takagi S, Chow L. Effects of calcium phosphate nanoparticles on Ca–PO_4 composite. J Dent Res 2007;86:378–83.
[7] Xu HH, Sun L, Weir MD, Takagi S, Chow LC, Hockey B. Effects of incorporating nanosized calcium phosphate particles on properties of whisker-reinforced dental composites. J Biomed Mater Res, B: Appl Biomater 2007;81:116–25.
[8] Zhao J, Liu Y, Sun W, Zhang H. Amorphous calcium phosphate and its application in dentistry. Chem Cent J 2011;5:40.
[9] Mehdawi I, Neel EAA, Valappil SP, Palmer G, Salih V, Pratten J, et al. Development of remineralizing, antibacterial dental materials. Acta Biomater 2009;5:2525–39.
[10] Chen Y-C, Ferracane JL, Prahl SA. Quantum yield of conversion of the photoinitiator camphorquinone. Dent Mater 2007;23:655–64.
[11] Calheiros FC, Daronch M, Rueggeberg FA, Braga RR. Influence of irradiant energy on degree of conversion, polymerization rate and shrinkage stress in an experimental resin composite system. Dent Mater 2008;24:1164–8.
[12] Gauthier M, Stangel I, Ellis T, Zhu X. Oxygen inhibition in dental resins. J Dent Res 2005;84:725–9.
[13] Palin WM, Fleming GJP, Trevor Burke FJ, Marquis PM, Randall RC. Monomer conversion versus flexure strength of a novel dental composite. J Dent 2003;31(July (5)):341–51.
[14] Charton C, Falk V, Marchal P, Pla F, Colon P. Influence of Tg, viscosity and chemical structure of monomers on shrinkage stress in light-cured dimethacrylate-based dental resins. Dent Mater 2007;23:1447–59.
[15] Sideridou ID, Achilias DS. Elution study of unreacted Bis-GMA, TEGDMA, UDMA, and Bis-EMA from light-cured dental resins and resin composites using HPLC. J Biomed Mater Res, B: Appl Biomater 2005;74:617–26.
[16] Gajewski VES, Pfeifer CS, Fróes-Salgado NRG, Boaro LCC, Braga RR. Monomers used in resin composites: degree of conversion, mechanical properties and water sorption/solubility. Braz Dent J 2012;23:508–14.
[17] Lempel E, Czibulya Z, Kunsági-Máté S, Szalma J, Sümegi B, Böddi K. Quantification of conversion degree and monomer elution from dental composite using HPLC and micro-Raman spectroscopy. Chromatographia 2014;77(17):1137–44.
[18] Reichl F-X, Simon S, Esters M, Seiss M, Kehe K, Kleinsasser N, et al. Cytotoxicity of dental composite (co)monomers and the amalgam component Hg^{2+} in human gingival fibroblasts. Arch Toxicol 2006;80:465–72.
[19] Goldberg M. In vitro and in vivo studies on the toxicity of dental resin components: a review. Clin Oral Invest 2008;12:1–8.
[20] Asmusen S, Arenas G, Cook WD, Vallo C. Photobleaching of camphorquinone during polymerization of dimethacrylate-based resins. Dent Mater 2009;25:1603–11.
[21] Khatri CA, Stansbury JW, Schultheisz CR, Antonucci JM. Synthesis, characterization and evaluation of urethane derivatives of Bis-GMA. Dent Mater 2003;19:584–8.
[22] Kleverlaan CJ, Feilzer AJ. Polymerization shrinkage and contraction stress of dental resin composites. Dent Mater 2005;21:1150–7.
[23] Al-Shekhli AAR, Al-Khfaji HH. Sorption and solubility of different light-activated composites. Int Dent 2008;8:56–61.
[24] Boaro LC, Gonçalves F, Guimarães TC, Ferracane JL, Pfeifer CS, Braga RR. Sorption, solubility, shrinkage and mechanical properties of "low-shrinkage" commercial resin composites. Dent Mater 2013;29:398–404.
[25] Palin WM, Fleming GJP, Burke FJT, Marquis PM, Randall RC. The influence of short and medium-term water immersion on the hydrolytic stability of novel low-shrink dental composites. Dent Mater 2005;21:852–63.

[26] Leung D, Spratt DA, Pratten J, Gulabivala K, Mordan NJ, Young AM. Chlorhexidine-releasing methacrylate dental composite materials. Biomaterials 2005;26:7145–53.
[27] Örtengren U, Wellendorf H, Karlsson S, Ruyter I. Water sorption and solubility of dental composites and identification of monomers released in an aqueous environment. J Oral Rehabil 2001;28:1106–15.
[28] Malacarne J, Carvalho RM, Mario F, Svizero N, Pashley DH, Tay FR, et al. Water sorption/solubility of dental adhesive resins. Dent Mater 2006;22:973–80.
[29] Nicolae LC, Shelton RM, Cooper PR, Martin RA, Palin WM. The effect of UDMA/TEGDMA mixtures and bioglass incorporation on the mechanical and physical properties of resin and resin-based composite materials. Conf Pap Sci 2014;2014:5.
[30] Zandinejad AA, Atai M, Pahlevan A. The effect of ceramic and porous fillers on the mechanical properties of experimental dental composites. Dent Mater 2006;22:382–7.
[31] Kendall K, Howard A, Birchall J, Pratt P, Proctor B, Jefferis S. The relation between porosity, microstructure and strength, and the approach to advanced cement-based materials [and discussion]. Philos Trans R Soc London, Ser A: Math Phys Sci 1983;310:139–53.
[32] Rodrigues Filho LE, Burger LAdS, Kenshima S, Bauer JRdO, Medeiros IS, Muench A. Effect of light-activation methods and water storage on the flexural strength of two composite resins and a compomer. Braz Oral Res 2006;20: 143–7.
[33] Anusavice K, Zhang N-Z, Shen C. Controlled release of chlorhexidine from UDMA–TEGDMA resin. J Dent Res 2006;85:950–4.
[34] Palmer G, Jones FH, Billington RW, Pearson GJ. Chlorhexidine release from an experimental glass ionomer cement. Biomaterials 2004;25:5423–31.
[35] Cheng L, Weir MD, Xu HHK, Kraigsley AM, Lin NJ, Lin-Gibson S, et al. Antibacterial and physical properties of calcium–phosphate and calcium–fluoride nanocomposites with chlorhexidine. Dent Mater 2012;28:573–83.
[36] Xia W, Razi MM, Ashley P, Neel EA, Hofmann M, Young A. Quantifying effects of interactions between polyacrylic acid and chlorhexidine in dicalcium phosphate-forming cements. J Mater Chem B 2014;2:1673–80.
[37] Marques MR, Loebenberg R, Almukainzi M. Simulated biological fluids with possible application in dissolution testing. Dissolution Technol 2011;18:15–28.